

Stone Stability in Non-uniform Flow

Nguyen Thanh Hoan¹, Marcel Stive², Rob Booij³, Bas Hofland⁴, Henk Jan Verhagen⁵,

Abstract

This paper presents the results of an experimental study on stone stability in flowing water. The various ways of quantifying the hydraulic loads exerted on the stones on a bed are extensively reviewed, verified and extended. As a result, a new stability parameter is proposed to better quantify the hydraulic loads exerted on the stones. A physical relationship between flow parameters and the bed damage - expressed as a stone transport formula - has been established for non-uniform flow. Such a relationship provides more consistent design criteria and allows an estimate of the cumulative damage over time which is important for making decisions regarding maintenance frequency and lifetime analysis of hydraulic structures.

Key words: Stone stability, stone transport, stone entrainment, incipient

¹Ph.D. student, Delft University of Technology, Hydraulic Engineering Section, P.O. Box 5048, 2600 GA Delft, The Netherlands. Presently: lecturer, Hanoi University of Civil Engineering, Faculty of Hydraulic Engineering, 55 Giai Phong street, Hanoi, Vietnam. Email: hoan@dongchay.com

²Professor, Delft University of Technology, Hydraulic Engineering Section, P.O. Box 5048, 2600 GA Delft, The Netherlands.

³Lecturer, Delft University of Technology, Environmental Fluid Mechanics Section, P.O. Box 5048, 2600 GA Delft, The Netherlands.

⁴Researcher, Deltares, Unit Hydraulic Engineering, P.O. Box 177, 2600 MH, Delft, The Netherlands.

⁵Associate Professor, Delft University of Technology, Hydraulic Engineering Section, P.O. Box 5048, 2600 GA Delft, The Netherlands.

motion, threshold condition, bed protection, bed damage, non-uniform flow, decelerating flow, open-channel flow.

1. Introduction

Despite the fact that many studies on the stability of stones in bed protections under flowing water have been conducted, our knowledge is still far from advanced and reliable. Issues like how to quantify the hydraulic loads exerted on the stones on a bed and how to assess the stability of the stones are central and most challenging in stone stability research.

Firstly, it is important that the hydraulic forces exerted on the stones in a bed are adequately quantified. A stability parameter - expressed as a dimensionless relationship between hydraulic loads and bed strength - is often used to quantify the influence of these forces on the bed. As the turbulence fluctuations of the flow are of importance for the stability of stones, their effect has to be taken into account, especially for non-uniform flow (Hoffmans and Akkerman, 1998; Pilarczyk, 2001; Jongeling et al., 2003; Hofland, 2005, among others). In the few studies available, no stability parameters have proven to be adequate in quantifying the influence of hydraulic loads exerted on the bed for non-uniform flow.

Secondly, the method with which the stability of stones is assessed also plays an important role. Available stability formulae used to determine stone sizes and weights are mainly based on the concept of incipient motion of bed material (see Buffington and Montgomery, 1997, for a review). Due to the stochastic nature of bed material movement, a robust flow condition at which the stones begin to move does not exist. Therefore, the threshold of

movement is a rather subjective matter and the stone stability assessment method based on it often yields inconsistent design criteria (Paintal, 1971; WL|Delft Hydraulics, 1972; Hofland, 2005). In contrast, the stability assessment method based on the stone transport concept leads to a result with a cause-and-effect relationship between flow parameters and the bed response, see Eq. (1) . Such a relationship provides consistent and more reliable design criteria and allows an estimate of the cumulative damage over time which is important for making decisions regarding maintenance frequency and life-time analysis of hydraulic structures (Mosselman et al., 2000; Hofland, 2005). Surprisingly, most of the previous studies on stone stability are restricted to the stability threshold concept and few have attempted to derive stone transport formulae. As a result, no physical relationship between the hydraulic load and the bed response is available for non-uniform flow.

These two challenging issues are dealt with in this paper. The objectives of the study are (i) to increase insight into the effect of hydraulic parameters, such as the velocity and the turbulence fluctuations, on the stability of stones in bed protections, (ii) to establish physical relationships between the hydraulic parameters and the bed damage (i.e., stone transport formulae) for non-uniform flow to obtain a reliable estimate of bed damage.

2. Review of literature

A cause-and-effect relationship between flow and its induced bed damage can be expressed as:

$$\Phi = f(\Psi) \tag{1}$$

where Ψ is a stability parameter and Φ is a bed damage indicator.

Stability parameters. Three available stability parameters that can be used to quantify the influence of the hydraulic loads exerted on a bed are those of Shields (1936), Jongeling et al. (2003) and Hofland (2005). The Shields stability parameter is expressed as:

$$\Psi_s = \frac{\tau_b}{\rho\Delta gd} = \frac{u_*^2}{\Delta gd} \quad (2)$$

in which d is the stone diameter, $\Delta = (\rho_s/\rho_w - 1)$, ρ_s is the stone density, ρ_w is the water density, g the gravitational acceleration, τ_b is the bed shear stress, and u_* is the shear velocity.

The Shields stability parameter was developed for uniform flow conditions and utilizes only the bed shear stress to quantify the flow forces. Turbulence fluctuations are not explicitly represented, but their effect is incorporated implicitly through empirical constants. This is a valid approach for uniform flows, for which the ratio of turbulence intensity to the shear velocity (and hence the bed shear stress) is virtually constant. In non-uniform flow, correction factors are conventionally applied to account for turbulence fluctuations and non-horizontal bottoms. This approach, however, does not physically incorporate the influence of the turbulence source in the upper high water column. Since the various correction factors are given rather arbitrary, it can only be used as a rule-of-thumb. Recently, Jongeling et al. (2003) and Hofland (2005) developed more generic approaches that utilize a combination of velocity and turbulence distributions over the water column to quantify the hydraulic loads. The Jongeling et al. stability parameter is expressed as:

$$\Psi_{WL} = \frac{\langle(\bar{u} + \alpha\sqrt{k})^2\rangle_{hm}}{\Delta gd} \quad (3)$$

where \bar{u} denotes the mean velocity, k denotes the turbulent kinetic energy,

$\alpha = 6$ is an empirical turbulence magnification factor, $\langle \dots \rangle_{hm}$ is a spatial average over a distance $hm = 5d + 0.2h$ above the bed, h is the water depth. The Hofland stability parameter reads:

$$\Psi_{Lm} = \frac{\max \left[\left\langle \bar{u} + \alpha \sqrt{k} \right\rangle_{Lm} \frac{Lm}{z} \right]^2}{\Delta g d} \quad (4)$$

where Lm denotes the Bakhmetev mixing length ($Lm = \kappa z \sqrt{1 - z/h}$), $\langle \dots \rangle_{Lm}$ is a moving average with varying filter length Lm , and z is the distance from the bed.

It is noted that the stones used in bed protections are often classified as a narrow grading, defined as $d_{85}/d_{15} < 1.5$ (CUR, 1995). The studies of Breusers (1965); Boutovski (1998) (flow), Van der Meer and Pilarczyk (1986); Van der Meer (1988, 1993) (waves) and others have revealed that the grading and the shape of stones practically have no influence on the stone stability when the nominal diameter d_{n50} is used as the characteristic dimension.

$$d_{n50} = \left(\frac{m_{50}}{\rho_s} \right)^{1/3} \quad (5)$$

where m_{50} is the mass of the median size of the stones (exceeded by 50% of stone weight).

Stones often move when an increased u -velocity fluid package reaches the bed (Hofland and Booij, 2004; De Ruijter, 2004). The probability that a high momentum fluid package reaches the bottom is related to flow parameters such as velocity and turbulence from higher up in the water column. Therefore, flow parameters at different depths can be used to represent the flow forces exerted on the bed. This was done in the stability parameters of Jongeling et al. (2003) and Hofland (2005). These parameters were developed to

explicitly account for the effect of turbulence in non-uniform flow. However, the appropriateness of these parameters has not been verified due to the high scatter level of the data that were used.

Bed damage indicator. A clearly defined and quantified measure of damage is essential for assessing the stability of a granular bed. The use of (dimensionless) bed load transport as a bed damage indicator (Φ) is conventional for uniform flow (e.g. Paintal, 1971). However, bed load transport is dependent on the upstream hydraulics; all the stones passing a certain cross section have been entrained upstream of this section. Bed load transport is therefore considered as a non-local parameter. Stability parameters are local parameters, making Eq. (1) a relationship of local and non-local parameters. Such a relationship can only be valid for uniform flow where the flow condition is unchanged along the channel. To adapt to various flow conditions, Hofland (2005) points out that the dimensionless entrainment rate (Φ_E) could be used as a bed damage indicator because it is completely dependent on the local hydrodynamic parameters. The dimensionless entrainment rate is expressed as

$$\Phi_E = \frac{E}{\sqrt{\Delta g d}} \quad \text{with} \quad E = \frac{nd^3}{AT} \quad (6)$$

in which n is the number of pick-ups per unit time (T) and area (A).

Although there has been much research on stone stability, the stone transport approach has rarely been applied. Two studies that used this approach are Paintal (1971, for uniform flow) and Hofland (2005, for non-uniform flow). The stone transport formulae developed by Paintal (1971) cannot be used for non-uniform flow because the flow forces are quantified by the Shields stability parameter (i.e., no turbulence effect) and the bed damage is quanti-

fied by the dimensionless bed load transport (i.e., non-local parameter). The tentative curve developed by Hofland (2005) describes the upper envelope of the highly scattered data of Jongeling et al. (2003) and De Gunst (1999). Therefore it does not reflect the actual relationship between the flow forces and the bed damage. As a result, no physical relationship between flow forces and bed damage is available for non-uniform flow.

To develop stone transport formulae for non-uniform flow, large amounts of data with detailed information on the hydraulic parameters and the corresponding bed damage are needed in order to give reliable conclusions. Such data are not available in the literature and therefore experimental work was conducted in this study.

3. Experiments

3.1. Experimental arrangements

The flow in gradually expanding open-channels and its influence on stone stability were focused on because under these conditions the turbulence intensity is high. The bed response (quantified by the dimensionless entrainment rate) and the flow field (velocity and turbulence intensity distributions) were measured in the experiments. The experimental installation is presented in Figure 1.

The experiments were undertaken in a laboratory open-channel flume with a length of 14.00 m, a height of 0.7 m and an available width of 0.5 m. The water is pumped through the flume from a central system in the laboratory and the water level is controlled at the downstream side using a manually controlled tailgate. To decelerate the flow, an expansion is made near the

end of the flume. To this end, the first part of the flume was narrowed at both sides. Then the extension was made by gradually increasing the width from the first segment to the width of the flume. By changing the expansion length (expansion angle), different combinations of velocity and turbulence can be obtained. Three different configurations⁶ with expansion angles α_E of 3, 5 and 7 degrees were built.

Figure 2 shows a schematic representation of the first experimental configuration indicating the location of the uniformly colored artificial stone strips. Natural stones having a density of 2700 kg/m^3 , a nominal diameter d_{n50} of 0.80 cm and d_{n85}/d_{n15} of 1.27 were used to create a 4-cm-thick rough and permeable bottom. The bottom was flat and the stones were angular, i.e. the edges were sharp, resembling stones used for bed protections. The flow velocity during the experiments was too low to displace the natural stones. To examine stone stability, two layers of uniformly colored strips of artificial light stones were placed at designated locations before and along the expansion (see Figure 3). These stones are made of epoxy resin with densities in the range of 1320 to 1971 kg/m^3 , mimicking shapes and sizes of natural stones. The artificial stones have a nominal diameter d_{n50} of 0.82 cm and d_{n85}/d_{n15} of 1.11.

A two-component, Laser Doppler Velocimetry (LDV) system was used, measuring u and w components of the velocity in the streamwise vertical plane. A light source Helium-Neon (HeNe) laser with a power of 15mW was used. The LDV uses the forward-scatter, reference-beam method. In the

⁶Also called *set-up* in all figures in this paper.

present study, a 400 mm lens was used, resulting in a measuring volume with dimensions of about 10 mm in spanwise direction and 1 mm in the other directions. Each time series lasted 2 minutes with a sampling frequency of 500 Hz. A detailed discussion on the choice of the signal length for one velocity measurement can be seen in Hoan (2008, Section 3.5).

Table 1 summarizes the hydraulic conditions measured in the experiment (see Figures 2 and 3 for profile location). More detailed descriptions of the experimental set-up, the choice of hydraulic conditions and stones used can be seen in Hoan (2008, chap. 3).

3.2. Experimental procedures

Since the measurements of the hydraulic conditions and the stone entrainment require different procedures, they were undertaken separately. Each series consists of five repetitive tests with the same flow conditions. The first test is dedicated to the measurements of the flow conditions while the next four tests are used to measure the stone entrainment data. The experimental procedure of one series was as follows.

In the first test of the series, the whole flume bottom was covered by only the natural stones, ensuring that no stones were displaced during the measurements. In this first run, the desired discharge was generated and the desired water depth was obtained by adjusting the weir at the downstream end of the flume. After the flow became stationary, the water level and the velocity could be measured. The LDV could measure the velocity as close as 3 mm from the bottom. The spacing between the measuring points Δz of 1 mm is applied for the first 5 measurements near the bottom and increases to 3 mm in the upper part of the inner region ($z/h < 0.2$). In the outer

region, the spacing between the measuring points increases towards the free surface with the maximum value of 15 mm. In total there are about 19 to 25 measuring points for each profile depending on the water depth. The number of measuring points in the inner region ($z/h < 0.2$) varies from 10 to 13.

After the hydraulic conditions were measured, the same flow condition was reproduced to measure the stone entrainment data. Uniformly colored strips of light artificial stones were placed at the designated locations. In order to obtain statistically reliable entrainment rate data, the entrainment test was repeated four times. The following procedure was applied to the entrainment test. A 30-minute initial settling period was applied prior to the actual test to remove loose stones that do not determine the strength of the bed. To start the actual entrainment test the flume was flooded slowly to the designated condition. After two hours, the flow was stopped and the number of displaced stones (the stones that are removed from their colored strips) was registered. The entrainment rates obtained from the four tests are averaged to obtain the entrainment rate for the series.

4. Experimental results

A detailed analysis of the flow results is presented in Hoan et al. (2007), Hoan (2007) and Hoan (2008, chap. 4), showing that the studied flow is considered non-uniform due to the deviation (and the high scatter level) of the turbulence intensity, the eddy viscosity and the mixing length from the theoretical and empirical curves reported for uniform flow. In this paper we try to make the link between governing flow parameters and the stability of bed protections in which the effect of turbulence is incorporated. The

various ways of quantifying the hydraulic loads exerted on the stones on a bed are verified and extended. The measured flow quantities and the stone entrainment data obtained from the experiment are used for the analysis. For a detailed presentation of the data, the reader is referred to Hoan (2007) and Hoan (2008, Appendix B). In this study, the theoretical wall level is set at δ position below the top of the roughness elements. The value of $\delta = 0.25d_{n50}$ was chosen (see Hoan, 2008, chap. 2 for a discussion).

4.1. *The proposed stability parameter*

In this section a new stability parameter which incorporates the influence of turbulence sources above the bed is proposed. A qualitative function is introduced to quantify the role of a turbulence source away from the bed. The formulation of the new stability parameter is based on the correlation analysis of the data measured in this study. The physical interpretation for this approach can be discerned from Figure 4 and is given below.

Let us assume that the flow force (F) exerted on a stone on the bed is proportional to the square of the near bed velocity (u) and the exposed surface area of the stone ($\propto d^2$):

$$F \propto \rho u^2 d^2 \quad (7)$$

Since the instantaneous flow velocity u can be expressed as $u = \bar{u} + u'$ (in which \bar{u} is the local, time-averaged component and u' is the fluctuating velocity component), the force can be expressed as

$$F \propto \rho(\bar{u} + u')^2 d^2 \quad (8)$$

From this we can estimate a *maximum* (extreme) force as

$$F_{max} \propto \rho[\bar{u} + \alpha\sigma(u)]^2 d^2 \quad (9)$$

where $\sigma(u) = \sqrt{u'^2}$ and α is a turbulence magnification factor which accounts for the influence of the velocity fluctuations.

If we assume that the turbulence source near the bed has the largest influence on stone stability on the bed and its influence gradually decreases to a negligible amount at a certain distance H from the bed ($H \leq h$), a weighting function f can be used to account for the influence of the turbulence source at a distance z (see also Figure 4):

$$f(z) = \left(1 - \frac{z}{H}\right)^\beta \quad (10)$$

where β is an empirical constant. The force from the water column H acting to move the stone can be averaged as follows:

$$\bar{F} \propto \frac{1}{H} \int_0^H \rho[\bar{u} + \alpha\sigma(u)]^2 d^2 \times \left(1 - \frac{z}{H}\right)^\beta dz \quad (11)$$

By dividing the moving force by the resisting force, i.e. the submerged weight of the stone $\equiv (\rho_s - \rho)gd^3$, a general form of a new Shields-like stability parameter can be derived:

$$\Psi_{u-\sigma[u]} = \frac{\left\langle [\bar{u} + \alpha\sigma(u)]^2 \times \left(1 - \frac{z}{H}\right)^\beta \right\rangle_H}{\Delta gd} \quad (12)$$

in which $\langle \dots \rangle_H$ denotes an average over the height H above the bed ($H < h$).

The suitability of a stability parameter representing the hydraulic loads exerted on a bed is evaluated by considering the correlation between the

stability parameter and the bed response. Therefore, the values of α , β , and H that give the best correlation between the new stability parameter and the dimensionless entrainment rate will be chosen to formulate the final expression of the new stability parameter.

4.2. Final formulation of the proposed stability parameter

The turbulence quantity used in the newly-proposed stability parameter is $\sigma(u)$. This turbulence component can be calculated directly from the instantaneous velocity data. To evaluate the new stability parameter, a correlation analysis was made for various possible values of α , β and H . The results are shown in Figure 5. The best correlation ($R^2 = 0.81$) is obtained when $\alpha = 3.0$, $\beta = 0.7$ and $H = 0.7h$. With $H > 0.7h$ the correlation is high, showing that large-scale structures are connected to the entrainment of bed material, which is consistent with the findings by Hofland (2005). The insensitivity to H/h (above 0.7) and β leads to a choice of the final form of the new stability as follows ($\alpha = 3$):

$$\Psi_{u-\sigma[u]} = \frac{\left\langle [\bar{u} + \alpha\sigma(u)]^2 \times \sqrt{1 - z/h} \right\rangle_h}{\Delta gd} \quad (13)$$

Figure 6 illustrates the role of each parameter in the new stability parameter. In this figure, the distributions of the key parameters in the new stability parameter are calculated using the measured flow quantities at profile 2 in series 2BR. It clearly shows the large influence of the turbulence in the new stability parameter.

The correlation between the new stability parameter and the measured entrainment rate is shown in Figure 7. The entrainment curve found by

regression analysis is given as ($R^2 = 0.81$, $\alpha = 3.0$)

$$\Phi_E = 9.6 \times 10^{-12} \Psi_{u-\sigma[u]}^{4.35} \text{ for } 7.5 < \Psi_{u-\sigma[u]} < 18 \quad (14)$$

4.3. Evaluation of the available stability parameters

In this section the stability parameters of Shields (1936), Jongeling et al. (2003) and Hofland (2005) are evaluated using the present data. A correlation analysis is made and the coefficient of determination gives the quantitative validity of these parameters.

In the analysis, the shear velocity in Eq. (2) was determined based on the measured Reynolds stress distribution. As only two velocity components (u - streamwise and w - upward) are available, the turbulent kinetic energy in Eqs. (3) and (4) was approximated by assuming that $\sigma(v) = \sigma(u)/1.9$. The approximation is based on the Electro Magnetic velocity Sensor (EMS) measurement of the flow conditions where both u - and v - velocity components were measured (see Hoan, 2008, Section 3.2.2 for a description). The analysis shows that there is virtually no correlation between Ψ_s and Φ_E for non-uniform flow (i.e., $R^2 = 0.18$). Therefore, the bed shear stress alone is not sufficient to quantify the flow forces acting on the bed. In contrast, the Jongeling et al. and Hofland stability parameters are strongly correlated to the entrainment parameter ($\alpha = 6$, $R^2 \approx 0.77$ for both). A sensitivity analysis of α in Ψ_{WL} and Ψ_{Lm} shows that $\alpha = 3.5$ (for Ψ_{WL}) and $\alpha = 3.0$ (for Ψ_{Lm}) give the best correlation. Based on the data measured in this study, a new stone transport formula for the modified stability parameter of Jongeling et al. (2003) is derived as ($R^2 = 0.82$, $\alpha = 3.5$):

$$\Phi_E = 1.16 \times 10^{-12} \Psi_{WL}^{4.57} \text{ for } 11 < \Psi_{WL} < 25 \quad (15)$$

A new stone transport formula for the modified stability parameter of Hofland (2005) is written as ($R^2 = 0.81$, $\alpha = 3.0$):

$$\Phi_E = 1.90 \times 10^{-8} \Psi_{Lm}^{4.32} \text{ for } 1.3 < \Psi_{Lm} < 3.2 \quad (16)$$

5. Discussion

In the foregoing sections, the velocity and entrainment data obtained from the present experiment were analyzed. Our aims are to (i) evaluate the performance of the Shields (1936), the Jongeling et al. (2003), the Hofland (2005) and the newly proposed stability parameter, and (ii) establish robust stone transport formulae which can be used to predict bed damage. The present approach can be extended to the study of sediment transport provided that the movement of the sediment on the bed is accurately quantified for non-uniform flow conditions.

It is noted that the present data have certain advantages over the existing data. To the author's knowledge, of the few studies on stone transport, this study probably carried out the most detailed and accurate velocity measurements, especially in the inner region ($z/h < 0.2$). With the LDV instrument, the velocity was measured very close to the bottom (3mm) with a small measuring volume, a high sampling frequency ($f = 500Hz$) and no flow disturbance. In Jongeling et al. (2003) and De Gunst (1999), with the water depth varying from 25 to 50 cm, only (10 - 12) measuring points were used to measure velocity profiles (compared to (12 - 19) cm water depth and (19

- 25) measuring points in the present study). Velocity measurements were not needed to formulate the stone transport formulae in the investigation of Paintal (1971) since the bed shear stress was calculated using the energy slope. In the present study, the entrainment tests were repeated four times. The entrainment rates obtained from the four runs were averaged to get a statistically reliable entrainment rate for the series.

5.1. Data comparison

In this section, the present data and those of Jongeling et al. (2003, next: WL) and De Gunst (1999, next: DG) are compared. Various flow configurations were used in the experiments of Jongeling et al. (2003) and De Gunst (1999), including the flows through horizontal bottoms (uniform flow), a long sill, a short sill, a gate and a backward-facing step (see Hofland, 2005, page 146 for a detail description). The WL and DG data were obtained from Figure 8.11 of Hofland (2005) with the following quantities: Ψ_{WL} (with $\alpha = 6$), Ψ_{Lm} (with $\alpha = 6$) and Φ_E . The comparison is plotted in Figure 8, showing a much larger scatter level in the WL and DG data. It appears that the present data had higher values of the stability parameters compared to those in the WL data, resulting in the larger entrainment rate. For both comparisons the present data are in good agreement with the WL and DG data. From Figure 8 we can conclude that Eqs. (14), (15) and (16) can also be used to predict entrainment rate outside the range of the present experiment, i.e. at a much lower entrainment rate (e.g. Φ_E of 10^{-9}).

5.2. Comparison of the stability parameters

The analysis presented in this paper has quantitatively confirmed that the use of the bed shear stress as the only quantity representing the flow forces is not sufficient for non-uniform flow conditions. This explains the low correlation between the Shields stability parameter (Ψ_s) and the dimensionless entrainment rate (Φ_E).

Conversely, the approaches that use the combination of velocity and turbulence distributions over a certain water column above the bed perform well. Three stability parameters that use these approaches are the Jongeling et al. (Ψ_{WL} , average of the extreme forces), the Hofland (Ψ_{Lm} , maximum of the extreme forces) and the newly-developed ($\Psi_{u-\sigma[u]}$, weighting average of the extreme forces) parameters. A graphical comparison of the four stability parameters is given in Figure 9. In this figure, $\langle x \rangle_H$ denotes a spatial average of x over a distance H .

The correlation analysis shows that the proposed stability parameter performs better than the stability parameters of Jongeling et al. (2003) and Hofland (2005) (i.e., $R^2 = 0.81$ vs. $R^2 = 0.77$). The analysis reveals that the difference in performance of the three stability parameters is not only due to the difference in quantifying the flow forces, but mainly because of the differences in quantifying turbulence (i.e., α). Once appropriate values of the turbulence magnification α are used, the three stability parameters perform similarly.

Surprisingly, the three approaches using the maximum (Ψ_{Lm}), average (Ψ_{WL}) and weighting average ($\Psi_{u-\sigma[u]}$) of the extreme forces over a water column above the bed appear to give similar results. This can be explained

by i) the insensitivity (of the correlation coefficient) to H/h (above 0.5) and β (Figure 5) and ii) the correlation between the maximum and the (weighting) average of the extreme forces.

It is noted that in the present analysis only the newly-proposed stability parameter can be directly calculated from the measured data. The stability parameters of Jongeling et al. (2003) and Hofland (2005) were calculated using the approximated turbulent kinematic energy discussed in the previous section.

6. Conclusions

From the analysis presented in this paper, the following conclusions can be drawn. Because (i) a variety of flow conditions is used in the present experiments and (ii) the present data are in good agreement with those of Jongeling et al. (2003) and De Gunst (1999), which used different flow configurations, stone sizes and densities, we believe that the present results are representative for general bed protections.

The analysis reported herein indicates that the Shields stability parameter is not sufficient for presenting the flow forces acting on the bed in non-uniform flow. The correlation of the Shields stability parameter to the entrainment deteriorates when the flow is more non-uniform. Conventional turbulence correction for non-uniform flow should not be used as it does not physically explain the influence of a turbulence source from the water column above the bed. In non-uniform flow, a different approach should be used to quantify the flow forces acting on the bed.

The formulation of the newly-proposed stability parameter has physi-

cally explained and quantitatively described the impact of flow (velocity and turbulence) on stone stability. This provides valuable insight into the understanding of the influence of the different flow quantities on stone stability. The high correlation of the proposed stability parameter [Eq. (12)] to the entrainment rate when the flow parameters at high water column are used indicates the role of large-scale flow structures. This confirms the finding by Hofland (2005) about the importance of large flow structures to stone stability. Based on the physical analysis and practical considerations, the final expression for the new stability parameter was formulated, expressed as Eq. (13). This stability parameter properly quantifies the flow forces acting on the bed.

For the first time since proposed by Jongeling et al. (2003), the approach that uses a combination of velocity and turbulence distributions to quantify the flow forces is verified by reliable data. The analysis indicates that different turbulence factors should be used for Jongeling et al. ($\alpha = 3.5$) and Hofland ($\alpha = 3.0$) stability parameters instead of $\alpha = 6$. The proposed stability parameter and the modified stability parameters of Jongeling et al. (2003) and Hofland (2005) perform similarly for the present data. This is explained by the insensitivity (of the correlation coefficient) to H/h (above 0.5) and β (Figure 5) and probably the correlation between the maximum and the (weighting) average of the extreme forces.

For the first time, the actual relationship between the flow and the stone stability has been established for non-uniform flow. This relationship is described by stone transport formulae developed using the newly-proposed stability parameter and the modified stability parameters of Jongeling et al.

(2003) and Hofland (2005), namely Eqs. (14), (15) and (16), respectively. These formulae can be used to predict the damage of bed protections (the applicability of using a numerical flow model together with these formulae to predict bed damage has been discussed in Hoan et al., 2008). Although similar correlations are found for the three stone transport formulae, Eq. (14) was developed using purely measured data while Eqs. (15) and (16) were based on the approximated turbulent kinematic energy data. Therefore, Eq. (14) is recommended with the alternatives being Eqs. (15) and (16) when only velocity u and turbulent kinematic energy k are available.

Since a good collapse of the data is obtained for a variety of stone densities (varying from 1320 to 1970 kg/m³), the influence of stone density is well incorporated into the formulae. Therefore, the newly-developed stone transport formulae are likely to be valid for other bed materials with different densities, including natural stones.

Critical values of $\Psi_{u-\sigma[u]}$, Ψ_{WL} and Ψ_{Lm} - translated from a subjectively chosen low value of Φ_E using (14), (15) and (16), respectively - should be used as design criteria to determine stone size in designing a bed protection. For instance, if $\Phi_E = 10^{-9}$ is chosen as a critical entrainment rate, the corresponding critical values of these stability parameters are $\Psi_{u-\sigma[u],c} = 2.9$, $\Psi_{WL,c} = 4.4$ and $\Psi_{Lm,c} = 0.5$. The required stone diameter can be determined as

$$d_{n50} = \frac{\langle [\bar{u} + \alpha\sigma(u)]^2 \times \sqrt{1 - z/h} \rangle_h}{\Delta g \Psi_{u-\sigma[u],c}} \quad (17)$$

$$d_{n50} = \frac{\langle (\bar{u} + \alpha\sqrt{k})^2 \rangle_{hm}}{\Delta g \Psi_{WL,c}} \quad (18)$$

$$d_{n50} = \frac{\max \left[\left\langle \bar{u} + \alpha \sqrt{k} \right\rangle_{L_m} \frac{L_m}{z} \right]^2}{\Delta g \Psi_{L_m, c}} \quad (19)$$

where $\alpha = 3.0; 3.5$ and 3.0 , respectively.

Acknowledgment

This research has been financially supported by the Ministry of Education and Training of Vietnam and Delft University of Technology. This financial support is gratefully acknowledged. The authors are grateful to Wim Uijtewaal, Sander de Vree of Environmental Fluid Mechanics Section of Delft University of Technology for their support and help during the experimental work.

References

- Boutovski, A. (1998). *Stabiliteit van gestorte steen*. M.Sc. thesis, Delft University of Technology. In Dutch.
- Breusers, H. N. C. (1965). Gradual closure VI, influence of shape and grading on the stability of riprap. Technical Report M731,WL|Delft Hydraulics. In Dutch.
- Buffington, J. M. and Montgomery, D. R. (1997). A systematic analysis of eight decades of incipient motion studies, with special reference to gravel-bedded rivers. *Water Resources Research*, 33(8): 1993-2029.
- CUR (1995). Manual on the use of rock in hydraulic engineering. Technical Report 169, Center for Civil Engineering Research and Codes, Gouda, The Netherlands.

- De Gunst, M. (1999). *Stone stability in a turbulent flow behind a step*. M.Sc. thesis, Delft University of Technology. (in Dutch).
- De Ruijter, R. (2004). *Turbulence structures affecting stone stability in backward-facing step flow (subtitle: Experiments by means of Particle Image Velocimetry)*. M.Sc. thesis, Delft University of Technology.
- Hoan, N. T. (2007). *Influence of turbulence on stone stability: report on measurement data (or Experimental data on Stone Stability under non-uniform flow)*. In Communications on Hydraulic and Geotechnical Engineering ISSN: 0169-6548 07-1, Delft University of Technology. <http://repository.tudelft.nl>
- Hoan, N. T. (2008). *Stone stability under non-uniform flow*. Ph.D. thesis, Delft University of Technology. www.library.tudelft.nl
- Hoan, N. T., Booij, R., Hofland, B., Stive, M.J.F., and Verhagen, H. J. (2008). Estimation of bed protection damage using numerical flow modeling. In *The Seventh International Conference on Coastal and Port Engineering in Developing Countries*, Dubai, UAE.
- Hoan, N. T., Booij, R., Stive, M. J., and Verhagen, H. J. (2007). Decelerating open-channel flow in a gradual expansion. In *The Fourth International Conference on Asian and Pacific Coasts*, Nanjing, China.
- Hoffmans, G. J. C. M. and Akkerman, G. (1998). Influence of turbulence on stone stability. In *The Seventh International Conference on River Sedimentation*, Hong Kong.

- Hofland, B. (2005). *Rock & roll: turbulence-induced damage to granular bed protections*. Ph.D. thesis, Delft University of Technology. www.library.tudelft.nl
- Hofland, B. and Booij, R. (2004). Measuring the flow structures that initiate stone movement. In *River Flow 2004*, pages 822-831. Routledge.
- Jongeling, T., Blom, A., Jagers, H., Stolker, C., and Verheij, H. (2003). Design method granular protections. Technical report Q2933 / Q3018, WL|Delft Hydraulics. In Dutch.
- Mosselman, E., Akkerman, G. J., Verheij, H., Hoffmans, G., Jongeling, T., and Petit, H. (2000). Stone stability, progress report. Technical Report Q2539, WL|Delft Hydraulics.
- Paintal, A. S. (1971). Concept of critical shear stress in loose boundary open channels. *Journal of Hydraulic Research*, 9(3): 91-113.
- Pilarczyk, K. (2001). Unification of stability formulae for revetments. In *Prog. XXIX IAHR congress*, Beijing.
- Shields, A. (1936). *Anwendung der Aehnlichkeitsmechanik und der Turbulenzforschung auf die Geschiebebewegung*. Mitteilungen der Preussischen Versuchsanstalt fur Wasserbau und Schiffbau, Heft 26, Berlin. in German.
- Van der Meer, J. W. (1988). *Rock slopes and gravel beaches under wave attack*. Ph.D. thesis, WL|Delft Hydraulics.
- Van der Meer, J. W. (1993). Conceptual design of rubble mound breakwaters. Technical Report 483, WL|Delft Hydraulics.

Van der Meer, J.W. and Pilarczyk, K. (1986). Dynamic stability of rock slopes and gravel beaches. In *The 20th International Conference on Coastal Engineering*, Taipei.

WL|Delft Hydraulics (1972). Systematisch onderzoek naar twee- en driedimensionale ontgroningen. Technical report, WL|Delft Hydraulics. In Dutch.

Notation

The following symbols are used in this paper:

A = area

B = width (of flume)

d = stone, particle diameter

d_n = nominal stone diameter ($\equiv \sqrt[3]{V}$)

d_{n50} = median nominal diameter ($\equiv \sqrt[3]{m_{50}/\rho_s}$)

E = entrainment rate

f = weighing function ($\equiv (1 - z/H)^\beta$)

F = flow force

F_{max} = (estimate of) maximum (extreme) occurring force

Fr = Froude number ($\equiv U/\sqrt{gh}$)

g = gravitational acceleration

h = water depth

H = water column height above the bed

k = turbulence kinetic energy

n = number of displaced stones

q_s = bed load transport per m width

Q = discharge

R = hydraulic radius ($\equiv \omega/\chi$)

R^2 = coefficient of determination

Re = Reynolds number ($\equiv Uh/\nu$)

Re_* = particle Reynolds number ($\equiv u_*d_n/\nu$)

T = period, time-scale or duration

u = streamwise velocity

u_* = shear velocity ($\equiv \sqrt{\tau_b/\rho}$)

w = upward velocity

x = coordinate in direction of flow

y = transverse coordinate

z = vertical coordinate

α = empirical constant

α_E = expansion angle

β = empirical constant

δ = boundary layer thickness

Δ = specific submerged density of stone ($\equiv \rho_s/\rho - 1$)

ρ = density of water

ρ_s = density of stone

τ = shear stress

τ_b = near bed shear stress

τ_c = critical near bed shear stress

Φ = transport parameter (bed damage indicator)

Φ_E = entrainment parameter (dimensionless entrainment rate)

Φ_q = dimensionless bed load transport

Ψ = stability parameter (ratio of load to strength)

Ψ_c = critical stability parameter

Ψ_{Lm} = Hofland stability parameter

$\Psi_{Lm,c}$ = critical value of Ψ_{Lm}

$\Psi_{u-\sigma[u]}$ = stability parameter using u and $\sigma[u]$

$\Psi_{u-\sigma[u],c}$ = critical value of $\Psi_{u-\sigma[u]}$

Ψ_s = Shields stability parameter ($\equiv \tau_b/\Delta gd$)

$\Psi_{s,c}$ = critical Shields stability parameter

Ψ_{WL} = stability parameter developed at WL|Delft Hydraulics

$\Psi_{WL,c}$ = critical value of Ψ_{WL}

\bar{x} = temporal average of x

$\langle x \rangle$ = spatial average of x

x' = fluctuating part of x around \bar{x}

List of Figures

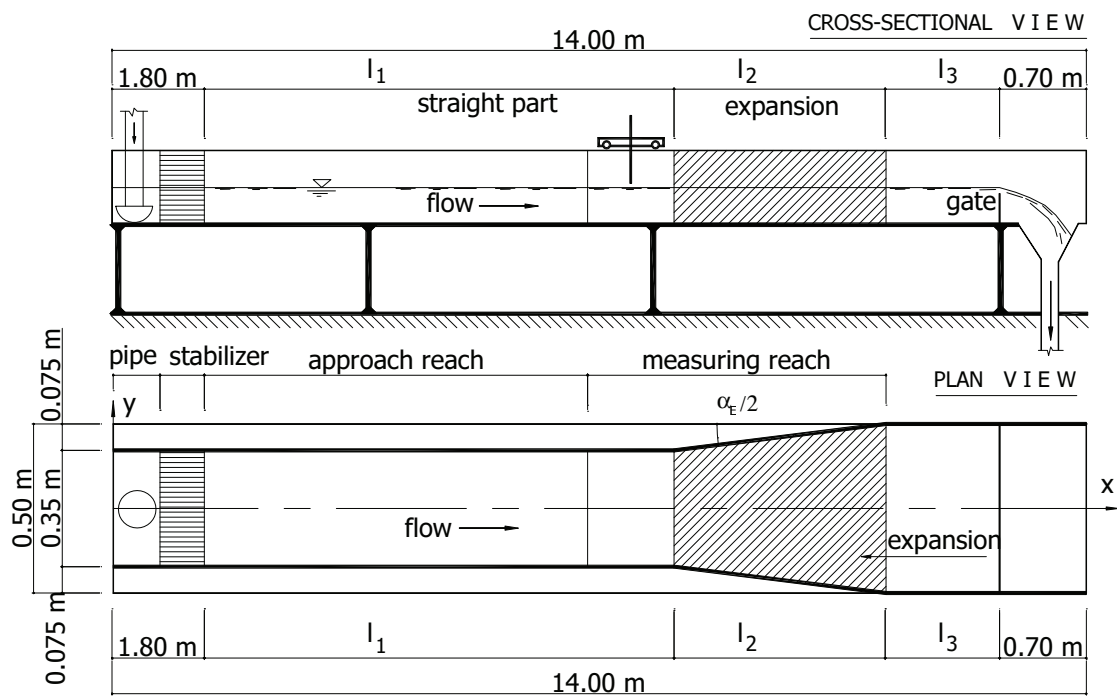
1	Experimental installation (not to scale).	29
2	The first experimental configuration indicating the placement of uniformly colored artificial stone strips (not to scale).	30
3	Longitudinal sections of the three experimental configurations.	30
4	The distributions of key parameters used to formulate the new stability parameter. From left to right: extreme force distribution (a), weighting function (b) and weighting average of the extreme forces (c).	31
5	Sensitivity analysis of α , β and H	31
6	Vertical distributions of key parameters in Eq. (13).	31
7	Measured $\Psi_{u-\sigma[u]}$ versus measured Φ_E	32
8	Data comparison. The α value of 6 was used for both Ψ_{WL} (top) and Ψ_{Lm} (bottom).	33
9	Typical distributions of the key parameters according to Eqs. (2), (3), (4) and (13).	34

List of Tables

1	Summary of hydraulic conditions measured from the experiments.	28
---	--	----

Table 1: Summary of hydraulic conditions measured from the experiments.

No	Series	Q	Profile 1			Profile 2			Profile 3			Profile 4		
			h	Re	Fr	h	Re	Fr	h	Re	Fr	h	Re	Fr
[-]	[-]	[l/s]	[cm]	[10 ⁴]	[-]	[m]	[10 ⁴]	[-]	[m]	[10 ⁴]	[-]	[m]	[10 ⁴]	[-]
1	1AR	22.0	11.7	6.2	0.498	12.1	5.5	0.423	12.1	5.2	0.394	12.3	4.9	0.362
2	1BR	20.0	12.0	5.7	0.439	12.1	5.0	0.385	12.2	4.7	0.357	12.3	4.4	0.331
3	1CR	23.0	13.0	6.5	0.448	13.0	5.7	0.396	13.2	5.4	0.363	13.3	5.1	0.338
4	1DR	26.5	13.9	7.5	0.466	14.3	6.6	0.395	14.5	6.2	0.363	14.5	5.9	0.343
5	1ER	24.0	13.9	6.8	0.422	13.9	6.0	0.371	14.1	5.6	0.344	14.3	5.3	0.316
6	1FR	27.0	15.0	7.6	0.425	14.8	6.7	0.381	15.2	6.3	0.346	15.3	6.0	0.323
7	1GR	31.0	15.7	8.8	0.456	16.1	7.7	0.385	16.2	7.3	0.361	16.2	6.9	0.338
8	1HR	28.0	15.8	7.9	0.407	15.9	7.0	0.355	16.2	6.6	0.324	16.5	6.2	0.299
9	1IR	31.5	17.0	8.9	0.412	17.1	7.9	0.359	17.4	7.4	0.329	17.8	7.0	0.300
10	1JR	35.5	17.9	10.0	0.428	18.1	8.9	0.372	18.3	8.3	0.343	18.5	7.8	0.318
11	1KR	32.0	18.0	9.1	0.383	18.1	8.0	0.333	18.3	7.5	0.308	18.5	7.1	0.287
12	1LR	35.5	19.0	10.0	0.391	19.1	8.9	0.343	19.1	8.3	0.321	19.3	7.8	0.298
13	2AR	22.0	11.6	6.2	0.507	11.6	5.6	0.459	11.6	5.1	0.419	11.8	4.7	0.379
14	2BR	20.0	12.0	5.7	0.442	11.9	5.1	0.401	11.8	4.7	0.373	11.8	4.3	0.341
15	2CR	23.0	12.8	6.5	0.459	12.6	5.8	0.420	12.7	5.4	0.382	12.9	5.0	0.345
16	2DR	26.5	13.8	7.5	0.471	13.8	6.7	0.424	13.7	6.2	0.391	13.9	5.7	0.355
17	2ER	24.0	13.2	6.8	0.458	13.2	6.1	0.409	13.3	5.6	0.373	13.3	5.2	0.343
18	2FR	27.0	14.4	7.6	0.448	14.1	6.9	0.418	14.2	6.3	0.379	14.3	5.8	0.345
19	2GR	31.0	16.0	8.8	0.443	15.9	7.9	0.402	15.9	7.2	0.368	16.1	6.7	0.335
20	2HR	28.0	15.9	7.9	0.404	15.8	7.1	0.367	15.9	6.5	0.332	15.9	6.0	0.308
21	2IR	31.5	16.9	8.9	0.413	16.7	8.0	0.379	16.6	7.3	0.350	16.8	6.8	0.318
22	2JR	35.5	17.5	10.0	0.442	18.0	9.0	0.382	17.9	8.3	0.351	18.1	7.6	0.320
23	2KR	32.0	17.8	9.1	0.390	17.9	8.1	0.347	17.8	7.5	0.320	17.9	6.9	0.293
24	2LR	35.5	18.6	10.0	0.405	18.2	9.0	0.375	18.5	8.3	0.335	18.6	7.6	0.306
25	3AR	22.0	12.1	6.2	0.474	12.6	5.4	0.393	12.8	4.8	0.343	-	-	-
26	3BR	20.0	12.0	5.7	0.438	12.7	5.0	0.351	13.0	4.4	0.303	-	-	-
27	3CR	23.0	12.9	6.5	0.454	13.3	5.7	0.379	13.4	5.1	0.333	-	-	-
28	3DR	26.5	13.8	7.5	0.474	14.4	6.6	0.387	14.7	5.8	0.332	-	-	-
29	3ER	24.0	14.1	6.8	0.411	14.7	5.9	0.340	15.0	5.3	0.292	-	-	-
30	3FR	27.0	14.9	7.6	0.428	15.5	6.7	0.355	15.6	5.9	0.310	-	-	-
31	3GR	31.0	15.7	8.8	0.456	16.4	7.7	0.373	16.8	6.8	0.319	-	-	-
32	3HR	28.0	15.8	7.9	0.406	16.4	6.9	0.336	16.6	6.2	0.294	-	-	-
33	3IR	31.5	16.9	8.9	0.412	17.8	7.8	0.335	17.5	6.9	0.305	-	-	-
34	3JR	35.5	17.5	10.0	0.442	18.0	8.8	0.370	18.5	7.8	0.316	-	-	-
35	3KR	32.0	17.7	9.1	0.391	18.0	7.9	0.335	18.2	7.0	0.292	-	-	-
36	3LR	35.5	18.3	10.0	0.414	19.2	8.8	0.336	19.5	7.8	0.293	-	-	-
37	3MR	36.0	12.4	10.2	0.752	11.8	8.9	0.710	12.7	7.9	0.562	-	-	-



Set-up 1: $\alpha_E = 3^\circ$, $l_1 = 7.60\text{m}$, $l_2 = 2.90\text{m}$, $l_3 = 1.00\text{m}$;

Set-up 2: $\alpha_E = 5^\circ$, $l_1 = 8.20\text{m}$, $l_2 = 1.70\text{m}$, $l_3 = 1.60\text{m}$;

Set-up 3: $\alpha_E = 7^\circ$, $l_1 = 8.20\text{m}$, $l_2 = 1.20\text{m}$, $l_3 = 2.10\text{m}$.

Figure 1: Experimental installation (not to scale).

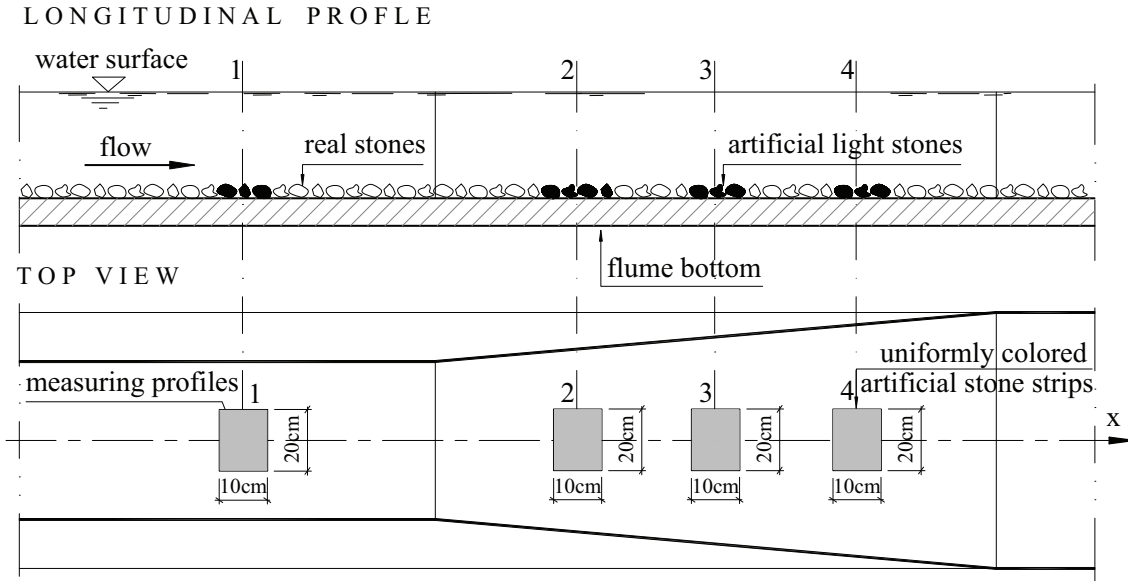


Figure 2: The first experimental configuration indicating the placement of uniformly colored artificial stone strips (not to scale).

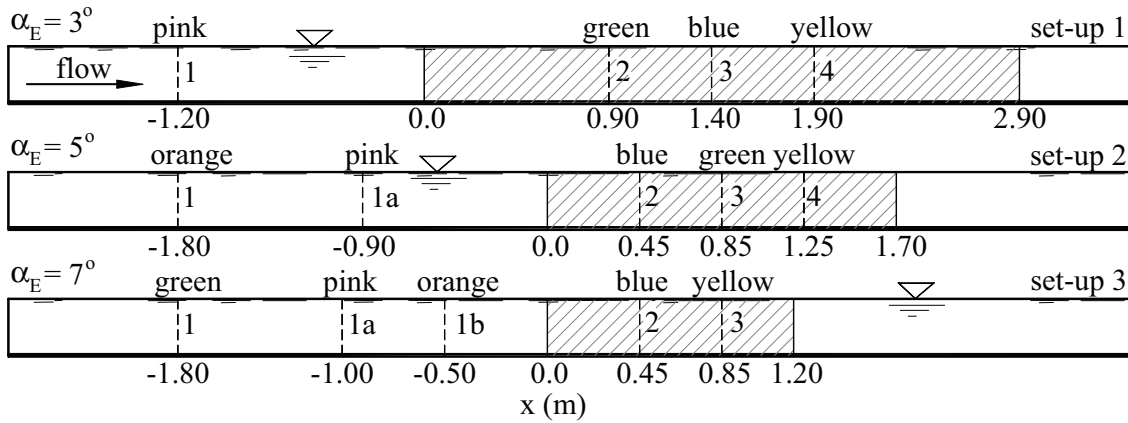


Figure 3: Longitudinal sections of the three experimental configurations. Hatched areas depict the expansion regions. Dashed lines are stone entrainment-measurement locations. The velocity was measured at profile 1, 2, 3 and 4. The stone colors are also indicated.

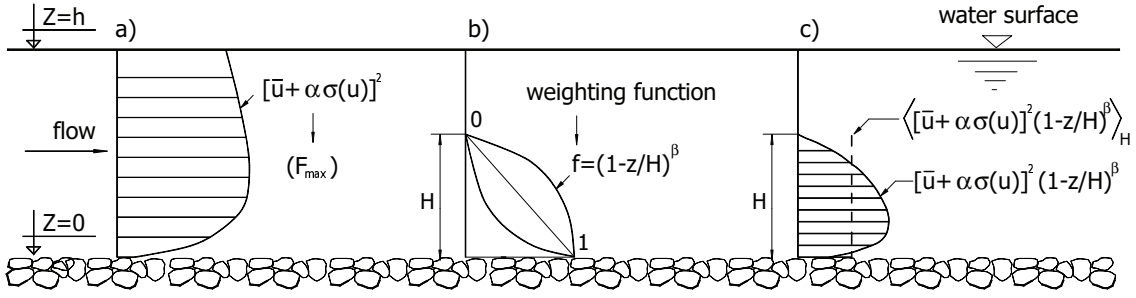


Figure 4: The distributions of key parameters used to formulate the new stability parameter. From left to right: extreme force distribution (a), weighting function (b) and weighting average of the extreme forces (c).

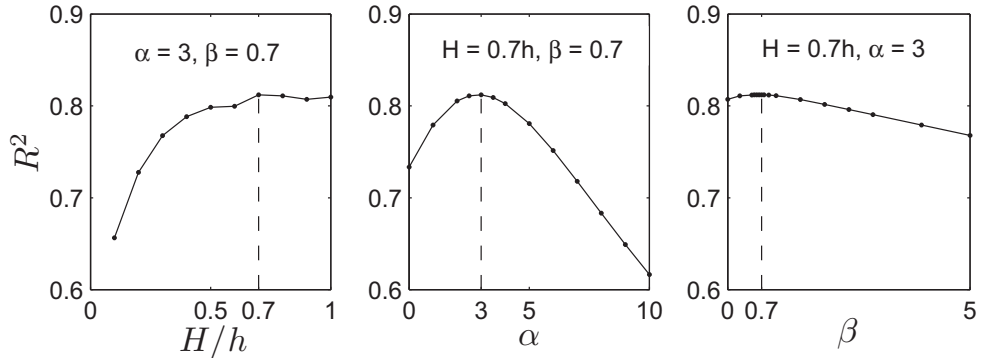


Figure 5: Sensitivity analysis of α , β and H .

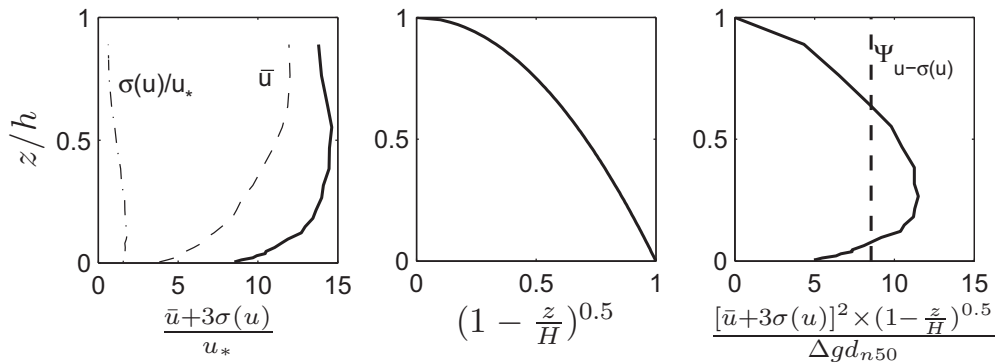


Figure 6: Vertical distributions of key parameters in Eq. (13).

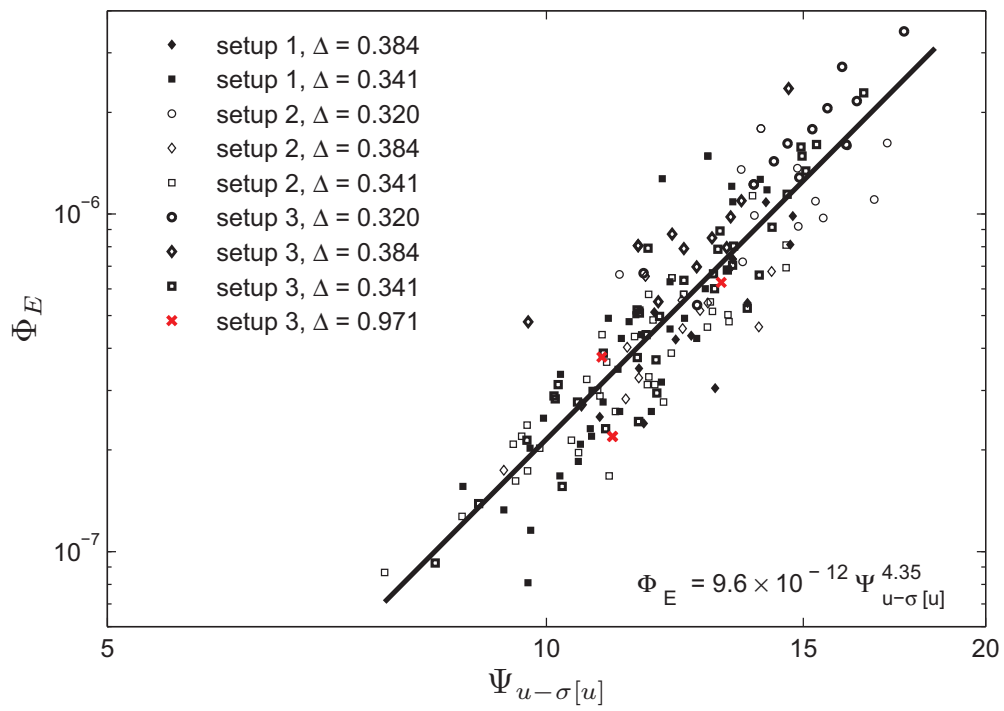


Figure 7: Measured $\Psi_{u-\sigma[u]}$ versus measured Φ_E .

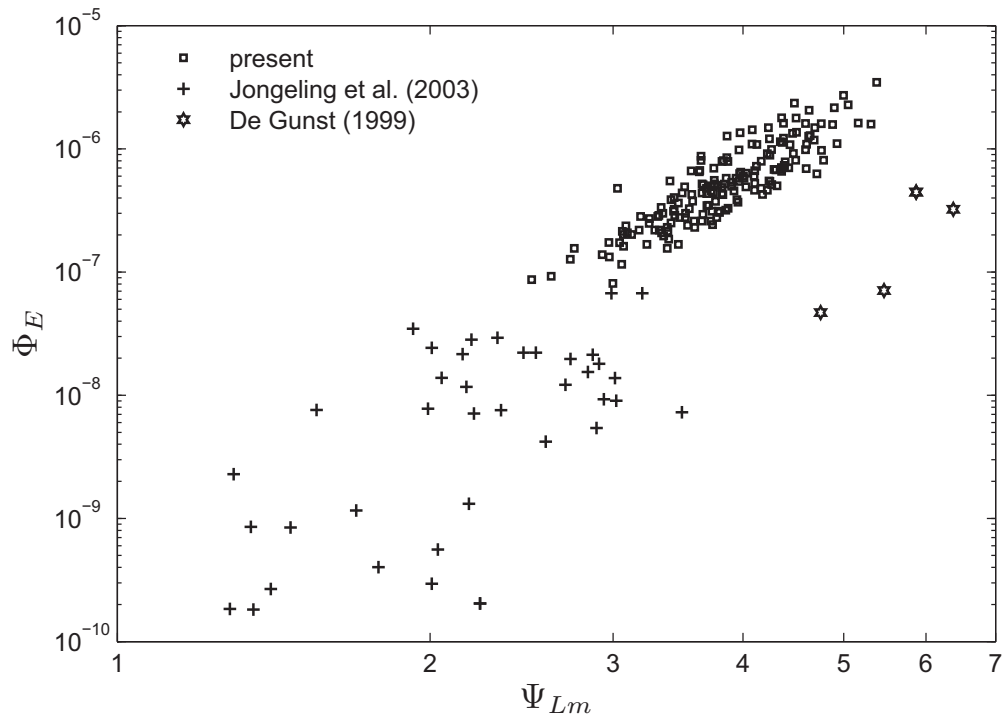
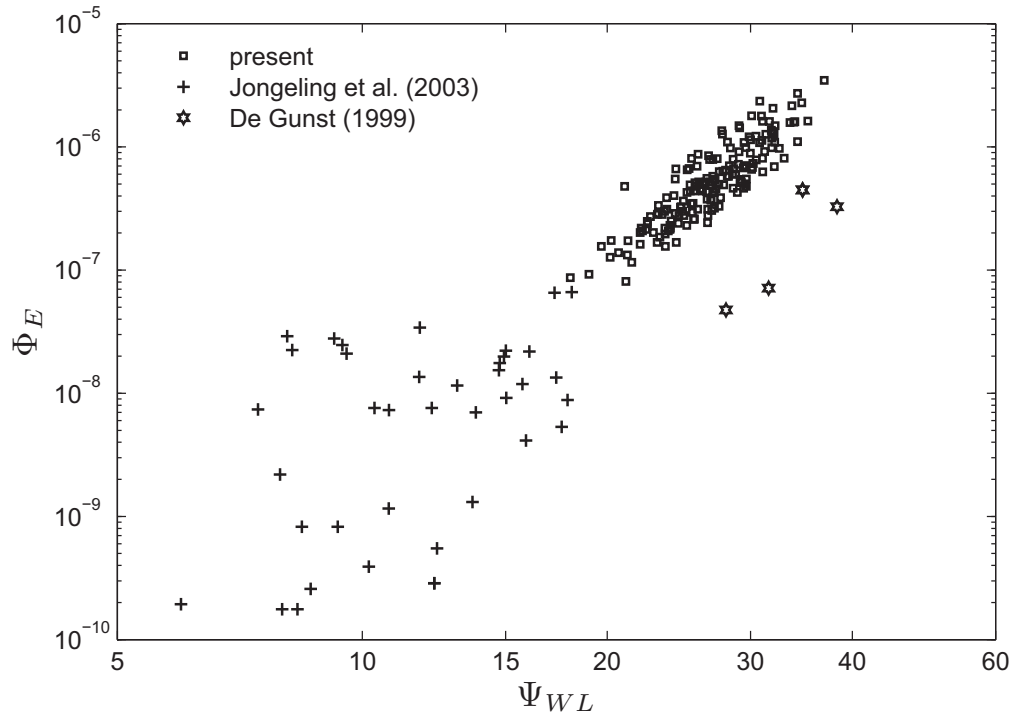


Figure 8: Data comparison. The α value of 6 was used for both Ψ_{WL} (top) and Ψ_{Lm} (bottom).

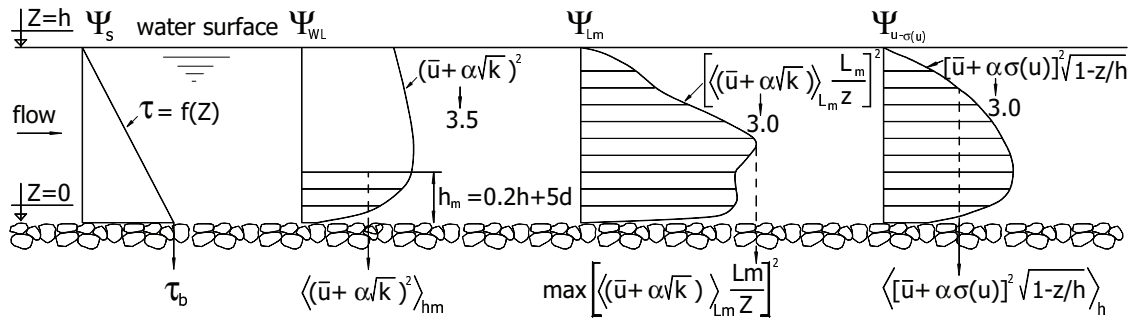


Figure 9: Typical distributions of the key parameters according to Eqs. (2), (3), (4) and (13).